

Interactions between Magnetite Oxidation and Flux Calcination during Iron Ore Pellet Induration

ANDREW R. FIRTH and JOHN F. GARDEN

Many chemical reactions take place simultaneously during the induration of iron ore pellets produced from magnetite concentrates. Two of the most important are magnetite oxidation and calcination of carbonate fluxes. The first reaction consumes oxygen diffusing into the pellet, while the second reaction produces carbon dioxide that must diffuse out of the pellet. A mathematical model combining the two reactions and gaseous diffusion within the pellet has been developed to quantify the interaction between the two reactions. This combined mathematical model showed that current induration plant mathematical models for the mass and energy balance around a pellet furnace are inaccurate in treating magnetite oxidation and flux calcination as separate reactions. Assuming separate reactions can lead to an error of up to 20 pct conversion of magnetite at the end of the preheat stage. This combined mathematical model, confirmed by experiments with single pellets, also demonstrated that calcination of fluxes also tends to follow a “shrinking core” model rather than reacting simultaneously across the pellet, as existing whole plant models assume. Modifying induration plant mathematical models in accordance with the findings of this article could lead to further savings in energy costs for pellet plants.

DOI: 10.1007/s11663-008-9162-6

© The Minerals, Metals & Materials Society and ASM International 2008

I. INTRODUCTION

MAGNETITE (Fe_3O_4) has been an important feedstock for the world steel industry for the last 50 years and will continue to be for the foreseeable future. The oxidation of magnetite is a reaction of great importance for the production of iron ore pellets due to its exothermic nature reducing the fuel requirements for their induration (heat hardening). Due to this fact, there have been many studies of the oxidation of ground magnetite rolled into pellets.^[1-5] The common consensus of the literature is that, on their own in an oxidizing environment, magnetite pellets oxidize following a “shrinking core” style reaction above 400 °C. This is due to the diffusion of oxygen to the reaction front through the porous matrix being the controlling resistance. As the temperature increases above 1300 °C, usually accompanied by a drop in oxygen potential in industrial pellet furnaces, the hematite product becomes less stable thermodynamically, and in extreme cases reversion to magnetite can occur. The presence of divalent ions such as calcium and magnesium in the magnetite lattice can also retard oxidation as they are incompatible with the corundum crystal structure of hematite.

Early magnetite oxidation studies^[1,2] were performed at a time when the majority of pellets being produced were “acid” pellets. Acid pellets do not have any fluxes, such as limestone, dolomite, or olivine, added to improve their metallurgical properties, and the gangue minerals present were typically quartz and bentonite clay. Over the 1990s, however, almost all pellets produced in the western world had fluxes added, especially carbonate fluxes such as limestone and dolomite. At a small number of deposits, “self-fluxing” of the magnetite concentrate occurs due to the presence of dolomite and calcite in the ore body, but this is rare. Carbonate fluxes generate CO_2 as they calcine, especially around 800 °C. The calcination reaction is thermally activated, so it occurs simultaneously across the pellet. This means that CO_2 is being generated and released from the fluxed pellet at the same time during firing that O_2 is trying to diffuse through the pellets to the oxidation interface. In previous mathematical models of the pellet induration process,^[6-8] however, the calcination and oxidation reactions are dealt with separately with no gas interaction assumed in the pellets.

In order to test the validity of the assumption that the gas generated during calcination does not affect oxidation, a mathematical model of a pellet undergoing induration has been developed using MATLAB.* This

ANDREW R. FIRTH is formerly Research Scientist, CSIRO Minerals. Contact e-mail: andrew.firth@corem.qc.ca JOHN F. GARDEN, Project Scientist, is with CSIRO Minerals, Pullenvale, Queensland, Australia.

Manuscript submitted May 25, 2007.

Article published online August 5, 2008.

*MATLAB is a trademark of Mathworks Inc., Natick, MA.

model includes both the calcination and oxidation reactions, as well as diffusion of gases within the pore

space of the pellet. Experiments using single pellets in a controlled gas atmosphere and heating rate were then used to validate the mathematical model and illustrate its conclusions.

II. EVIDENCE FOR GAS INTERACTION

The thermogravimetric analysis in air of a typical fluxed pellet feed can be seen in Figure 1. The temperature ramp for the 50 μg sample was 10 $^{\circ}\text{C}$ per minute. Figure 1 shows that the temperatures encountered by the pellets during the preheat stage of induration, oxidation of magnetite, and calcination of limestone and dolomite occurred simultaneously around 700 $^{\circ}\text{C}$.

It can be calculated from the mass of the added carbonate flux in a typical fluxed pellet^[9] that around 0.04 g of CO_2 is produced for each pellet (3.5 g total mass). At a temperature of 800 $^{\circ}\text{C}$, this is equivalent to 81.6 cm^3 of gas. Assuming that the CO_2 gas is evolved at a constant rate from the pellet over 6 minutes at this temperature, the generation rate of CO_2 from the pellet is 0.23 cm^3/s (2.58×10^{-5} mol/s). For a pellet of 12.5-mm diameter and a typical green pellet porosity of 0.3, the internal volume is 0.307 cm^3 . This estimate suggests that roughly 75 pct of the gas volume of the pellet in CO_2 (assuming atmospheric pressure) is released each second during calcination, more if the rate is more rapid. Simultaneously, oxygen is trying to diffuse through the pellet to the magnetite core. Papanastassiou and Bitsianes^[1] determined the effective diffusivity of oxygen in magnetite pellets (with no added carbonates) to be 0.259 cm^2/s at 1000 $^{\circ}\text{C}$. This finding results in a flow of oxygen into the pellet of the same order of magnitude (10^{-5} mol/s) as the rate of CO_2 generation. From this calculation and the observation that magnetite oxidation and flux calcination are occurring simultaneously in the pellet (Figure 1), it must be surmised that the CO_2 generation from calcination and its bulk flow from inside the pellet must affect the access of oxygen to the magnetite particles. The aim of this study is to quantify the degree of retardation for magnetite oxidation caused by simultaneous limestone calcination.

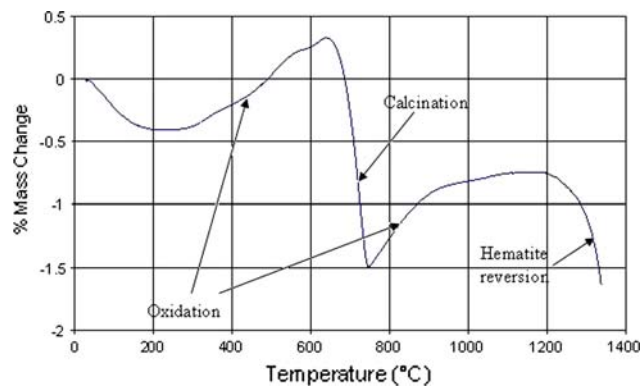


Fig. 1—Thermogravimetric analysis plot for a typical fluxed magnetite pellet feed including fluxes^[9].

III. MATHEMATICAL MODEL

A “method of lines” approach was used to solve the partial differential equations resulting from gaseous diffusion within the porous spaces in the pellet. Bulk flow due to pressure gradients in the pellet was included in the model as rapid calcination of limestone could generate significant pressure within the pellet. Thermal diffusion was also determined within the pellet using a diffusion coefficient determined for unfired iron ore pellets by the laser flash technique.^[10] This included the heats of reaction from the oxidation (exothermic) and calcination (endothermic), which were found to affect the progress of the reaction front. A single pellet, assumed to be a sphere of 12.5-mm diameter, was divided radially in an equidistant manner. The spatial derivatives were then approximated using a finite difference approach. The remaining ordinary differential equations in the time domain were solved for the time period required using a variable order numerical differentiation method.

A. Diffusion

The gas phase within the pellet and the surrounding atmosphere was assumed to be made up of three components: nitrogen, oxygen, and carbon dioxide. The method of Slattery and Bird^[11] was used to estimate the binary diffusivities between the three components. To translate these binary diffusivities to those that would apply in the ternary mixture of gases, the relationship developed by Curtis and Hirschfelder^[12] was applied. The Knudsen diffusion effects in the porous solid were modeled using the “dusty gas” model^[13] for uniformly sized spherical particles. The independent parameters for the dusty gas model are the diameter of the individual grains, the porosity of the pellet, and the tortuosity of the pores. An expression developed by Maizel *et al.*,^[14] relating the tortuosity to the porosity of green pellets, was used to connect these two parameters. Boucher and Wilhelm^[15] have also reported that green ball porosity can be slightly lower at the center of a pellet compared to the outside as it has undergone more compaction events during the growth phase, although the authors did not quantify the difference. It is acknowledged that, at firing temperatures, the porosity of magnetite pellets generally decreases due to sintering of the iron oxide grains, while the tortuosity would remain relatively constant. As this study is more concerned with preheat temperatures, below those at which pellet sintering becomes significant, it is expected that this relationship should be sufficient. The porosity of the magnetite pellets was assumed for the mean case to be 0.30, a typical value obtained from Wynnyckyj.^[16]

At the surface of the pellet, the boundary layer resistance of mass transfer to the pellet was modeled using a Sherwood number correlation. A constant Sherwood number of 4 was assumed, because the work of Papanastassiou and Bitsianes^[1] found that the typical Sherwood number in a packed bed of pellet varied only marginally between 4 and 4.5.

B. Reactions

The only two reactions that are modeled are oxidation of magnetite and calcination of limestone. Calcination of dolomite is a more complex, two-stage reaction, although the actual CO_2 production is nearly identical. The model for the calcination of limestone was based on the work of Borgwardt^[17] and Fuertes *et al.*,^[18] where a reversible Arrhenius equation was used, modified by the available surface area of limestone for reaction. The particle size of the limestone grains was assumed to be uniform and the same as the magnetite with the correlation to surface area taken from Borgwardt.^[17] The change in surface area as the reaction proceeded was modeled at each point in the pellet according to Eq. [1].^[18]

$$S = S_o(1 - X)^{2/3} \quad [1]$$

The oxidation of magnetite was modeled with the spherical fixed packed bed model presented by Papanastassiou and Bitsianes.^[19] This model was selected instead of the usual “shrinking core” approximation, because it could track the oxidation of magnetite in the individual concentric layers of the pellet. The deficiency of this model compared to the normal shrinking core model is that it is more computationally intensive. The base differential equations for the shrinkage in the magnetite core in each grain and the oxidation rate can be seen in Eqs. [2] and [3].

$$\frac{\partial r_g}{\partial t} = \frac{(C_{\text{O}_2,eq} - C_{\text{O}_2})}{\Delta\rho_o \left(\frac{r_g^2}{D_{ss}} \left(\frac{1}{r_g} - \frac{1}{r_{go}} \right) + \frac{1}{k_{ox}} \right)} \quad [2]$$

$$R_{ox} = \frac{3(1 - \varepsilon)(C_{\text{O}_2,eq} - C_{\text{O}_2})}{\left(\frac{r_{go}^3}{D_{ss}} \left(\frac{1}{r_g} - \frac{1}{r_{go}} \right) + \frac{r_{go}^3}{r_g^2 k_{ox}} \right)} \quad [3]$$

There is some uncertainty as to the appropriate values for the diffusion of oxygen through hematite to the reaction interface (D_{ss}) and the chemical reaction constant (k_{ox}) at that interface. This is due to magnetite oxidation at high temperatures normally being studied as a shrinking core reaction where oxygen diffusion through the pores is the limiting factor. The estimate for the chemical reaction constant was taken directly from Papanastassiou and Bitsianes^[1] for their results using taconite-derived magnetite concentrate pellets. The activation energy (2.49 kcal/mol) used in the model was that found for the initial oxidation rate at high temperature, before oxygen diffusion through the pellet became rate controlling. The overall magnetite oxidation rate is insensitive to small changes in this activation energy, because it is not rate controlling or influencing at high temperatures. This is consistent with the experimental observations of Monsen *et al.*, who showed that solid-state diffusion through the product hematite layer controlled the oxidation reaction in individual magnetite grains. Monsen *et al.*^[20] extrapolated an Arrhenius relationship for solid-state diffusion in the iron oxide

grains, by examining the oxidation of individual magnetite particles in air at temperatures up to 850 °C. The equilibrium concentration for oxygen used in the reversible reaction model for hematite-magnetite equilibria was calculated from thermodynamics. Modifying the thermodynamic equation for oxygen equilibrium to take into account magnesium dissolution^[21] into the magnetite was evaluated, but it was found to not have an appreciable effect on the oxidation rate.

IV. SINGLE PELLETT EXPERIMENTS

A 20-kg batch of green balls was prepared from an industrial magnetite concentrate in a balling drum (600-mm diameter, 220-mm depth, and rotating at 25 rpm). The target chemical analysis of the fluxed pellets (after firing) was 65.7 pct total Fe, 2.3 pct SiO_2 , 2.3 pct CaO, 1.4 pct MgO, and 0.14 pct Al_2O_3 , with 7 kg/t bentonite used as the binder. The total mass loss assuming full calcination and oxidation for these pellets was 0.63 pct. The magnetite concentrate and the fluxes were ground to 85 to 90 pct $-38 \mu\text{m}$. More details on the procedure producing the green balls can be found in Firth.^[9]

The green balls were heated using a QHC-E44 VHT infrared image furnace produced by Ulvac-Riko Inc. (Kanagawa, Japan). The furnace uses gold-plated parabolic mirrors to focus infrared radiation on the hot zone. The advantage of using this type of furnace is that rapid temperature changes can be precisely measured and controlled. Similar furnaces have found a use in fundamental studies of the reactions in iron ore sintering and have recently been used to study similar reactions in iron ore pellets.^[9,22,23] While preheated pellets can be sampled from pot grate experiments and industrial furnaces, there is some uncertainty as to the exact thermal history of these pellets. In the infrared image furnace, the temperature at which reactions occur can be determined and controlled with precision. The atmosphere of the furnace can also be controlled and quenching of the sample can be performed using nitrogen gas cooling lances. The use of nitrogen during cooling is important to stop the oxidation reaction of the magnetite at an intermediate stage.

Single green balls of a suitable size, close to 12.5 mm in diameter, were weighed then placed in a nickel foil container before being put into the rapid heating furnace. An R-type thermocouple (platinum-platinum-10 pct rhodium) was used to measure the surface temperature of the pellet. Once the pellet was in place, the surface temperature of the pellet was increased to 240 °C in 4 minutes and then to the desired preheat temperature (between 900 °C and 1100 °C) in 3 minutes. This heating profile to the desired preheat temperature was used to approximately simulate the temperature ramp experienced by pellets in the middle of a pellet bed in a reproducible way.

Ramping to the preheat temperature immediately would create unrealistic thermal profiles through the pellet. After the desired time period (between 0 and 3 minutes) at the preheat temperature, the heating was

terminated and the pellet was quenched immediately in a 100 L/min flow of nitrogen. Both the preheat time and preheat temperature were varied to provide a range of samples with which to compare the extent of the oxidation and calcination.

V. RESULTS

The results presented for the mathematical model assume a 7.45 pct limestone addition and a magnetite content of 90 pct in the pellets, both on a mass basis. This is equivalent to the composition of the iron ore pellets used in the experimental work, with the exception that the carbonates in the pellet are a mixture of limestone and dolomite with trace amounts of siderite (FeCO_3).

A. Isothermal Case

The results from the mathematical model for isothermal oxidation-calcination of a simulated iron ore pellet showed that the addition of limestone could significantly impact the oxidation process (Figure 2). At high temperatures (above 1100 °C) or at low temperatures (below 700 °C), there was little impact of the presence of carbonate on the oxidation rate of the magnetite. For temperatures in between, however, the time required for oxidation increased by up to 50 seconds when carbonate was present. The greatest difference in the degree of magnetite oxidation between the two cases was observed between 30 and 150 seconds after the start.

An initially surprising adjunct result, given that published pellet induration models^[6-8] treated calcination of carbonates as occurring simultaneously throughout the pellet, was that calcination of limestone also follows a shrinking core pattern. Upon further investigation of the results, it appears natural, however, as the interior of the pellet becomes saturated with CO_2 at the thermodynamic equilibrium partial pressure with the reaction becoming diffusion controlled. This correlates well with observations on calcination of large limestone particles of a similar size to iron ore pellets.^[24]

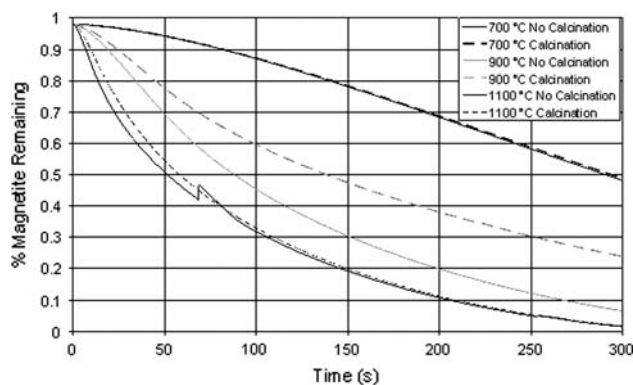


Fig. 2—Comparison of isothermal oxidation rates with or without simultaneous calcination of fluxes. Note that some numerical instability was observed in simulating the 1100 °C case for no calcination.

This result also suggests changes should be made to “whole plant” mathematical models for pellet induration, which typically assume that calcinations occurs simultaneously across the whole pellet.

Figure 3 illustrates the conversion over time for the whole pellet for both the oxidation and calcination reactions at three temperatures, 700 °C, 900 °C, and 1100 °C. At 1100 °C and above, the calcination reaction is very rapid with all the carbonate in the pellet consumed within 20 seconds (Figure 3(c)). Because this is much more rapid than the reaction rate for magnetite oxidation and because the carbon dioxide has diffused out of the pellet rapidly, there is no obstruction to oxygen diffusing to the shrinking core for the majority of

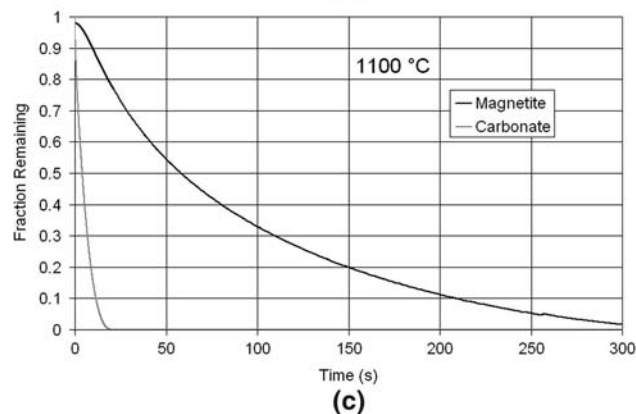
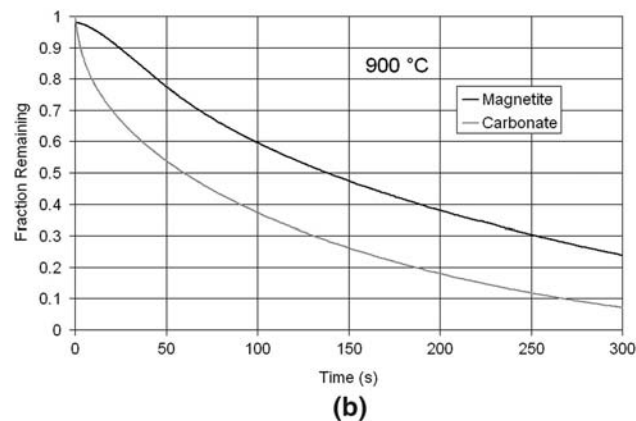
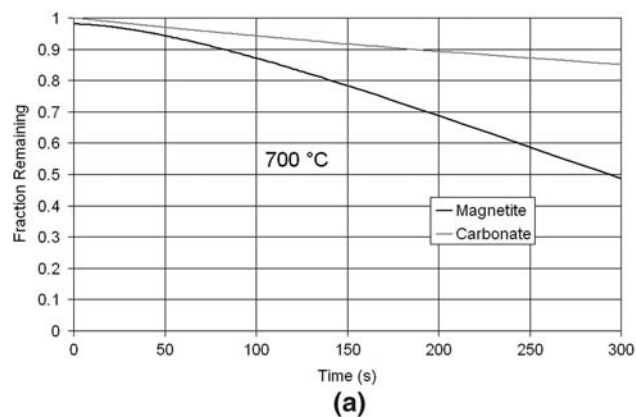


Fig. 3—Comparison of the progress of oxidation and calcination reactions at 700 °C, 900 °C, and 1100 °C.

the reaction period. At 700 °C and below (Figure 3(a)), the equilibrium partial pressure of CO₂ is relatively low, limiting the rate of the calcination reaction. The rate of magnetite oxidation is faster at this temperature, and the relatively low rate of CO₂ diffusing from the pellet provides little resistance to oxygen diffusing to its reaction interface. Where the reaction rates for calcination and oxidation are similar, for example, around 900 °C (Figure 3(b)), is where the most interaction occurs, and the buffeting effect of CO₂ diffusing out through the pellet on oxygen diffusing toward the oxidation front is most pronounced. Unlike the effect of carbonate calcination on magnetite oxidation, it was found that the inclusion of simultaneous magnetite oxidation had a negligible effect on the calcination rate of the fluxes compared to calcination in an equivalent inert matrix.

B. Drying and Preheat Profiles

Naturally, the firing of pellets is not an isothermal process and magnetite oxidation and flux calcination will occur across a range of temperatures. The interaction between flux calcination and magnetite oxidation during a pellet temperature ramp was performed, the ramp being identical to that used for preheat experiments in the infrared image furnace. In this way, comparison with experiments on fluxed pellets from those tests can be performed. Naturally, real pellet thermal histories follow more complex trajectories, but these are more difficult to describe mathematically. The results for a maximum preheat temperature of 1000 °C can be seen in Figure 4.

It can be seen that the presence of the carbonate significantly increases the length of time required for sufficient magnetite oxidation to occur. This follows the data from Firth,^[9] where the observed time required to completely oxidize the magnetite in the fluxed pellets was longer than that recorded by Papanastassiou and Bitsianes^[1] using acid magnetite pellets that contained no carbonate flux.

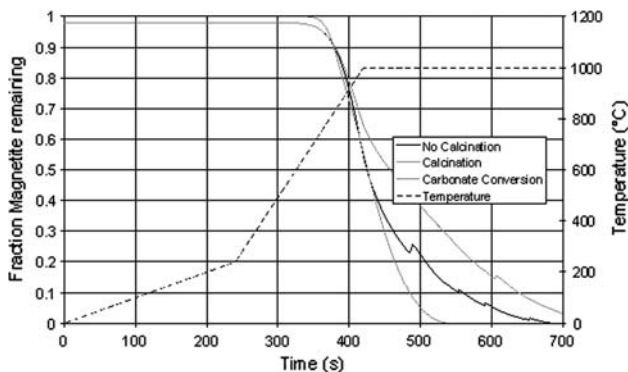


Fig. 4—Comparison of magnetite oxidation rate between fluxed and carbonate free pellets for a heating profile typical of a preheated pellet. The calcination rate for the fluxed pellet is also included. The sawtooth patterns on the oxidation curves are due to numerical instability in the simulation.

C. Experimental Validation of the Mathematical Model

To back up the results from the mathematical model, interrupted firing experiments were conducted on a single pellet using the infrared image furnace technique described earlier. A series of experiments were conducted where the pellet was preheated to a point where neither magnetite oxidation nor flux calcination was complete according to the mathematical model. The experimental levels of oxidation and calcination were then compared to the model. For oxidation, the comparison was made with optical micrographs of the pellet taken in reflected light. Hematite is white in reflected light, indicating a high reflectance, while magnetite is pink-gray in color as its spinel crystal structure has a lower reflectance. The black space surrounding the iron oxide grains can either be pores filled with epoxy resin, or less commonly silica particles, which have similar poor reflectance. The occasional milky gray particle in Figure 5 is carbonate flux. It should be noted that there was some hematite (around 5 pct) in the initial concentrate used to make the green balls. This initial hematite is different in appearance to hematite generated from magnetite oxidation, which initially penetrates the surface of the magnetite grain before expanding preferentially along the close-packed planes.^[20] The extent of penetration into the pellet of grain surface oxidation is marked in Figure 5 by a solid line across the micrographs. This penetration distance is equivalent to the experimental 0 pct conversion point marked in Figure 7. As the pellet temperature increases, the rate of surface oxidation of the magnetite grains in the pellet also increases. This limits the ability of oxygen to diffuse through the pore spaces and results in higher gas diffusion control of the oxidation reaction, leading to a sharper boundary between unoxidized magnetite grains and fully oxidized hematite.

The calcination front in terms of the start of carbonate loss was estimated from calcium element maps of the pellets obtained using electron probe microanalysis (EPMA). These calcium element maps can be seen in Figure 6. The calcination front in the pellets was assumed to be the point at which calcium begins to leave the calcined dolomite or calcite particles to form calcium ferrites by reacting with the surrounding iron oxides. Calcium oxide is highly reactive with the surrounding oxides, forming calcium ferrites and partially dissolving into the spinel structure of magnetite. This allows the calcium ions to become highly mobile once the carbonate component of the flux has been decomposed. On the element maps in Figure 6, the calcination front is taken to be the point where the large calcite particles are no longer at their original calcium concentration, which is represented as white, indicating that the calcium carbonate has decomposed and the remaining calcium oxide has started to react with the nearby iron oxides. This point is highlighted by a white line. Anything containing no calcium, for example, iron oxides remote to the flux particles or the pore spaces filled with epoxy, are shown as black. In large limestone particles over 1 mm in size, calcination has been proven to be controlled by diffusion of the product CO₂ gas out

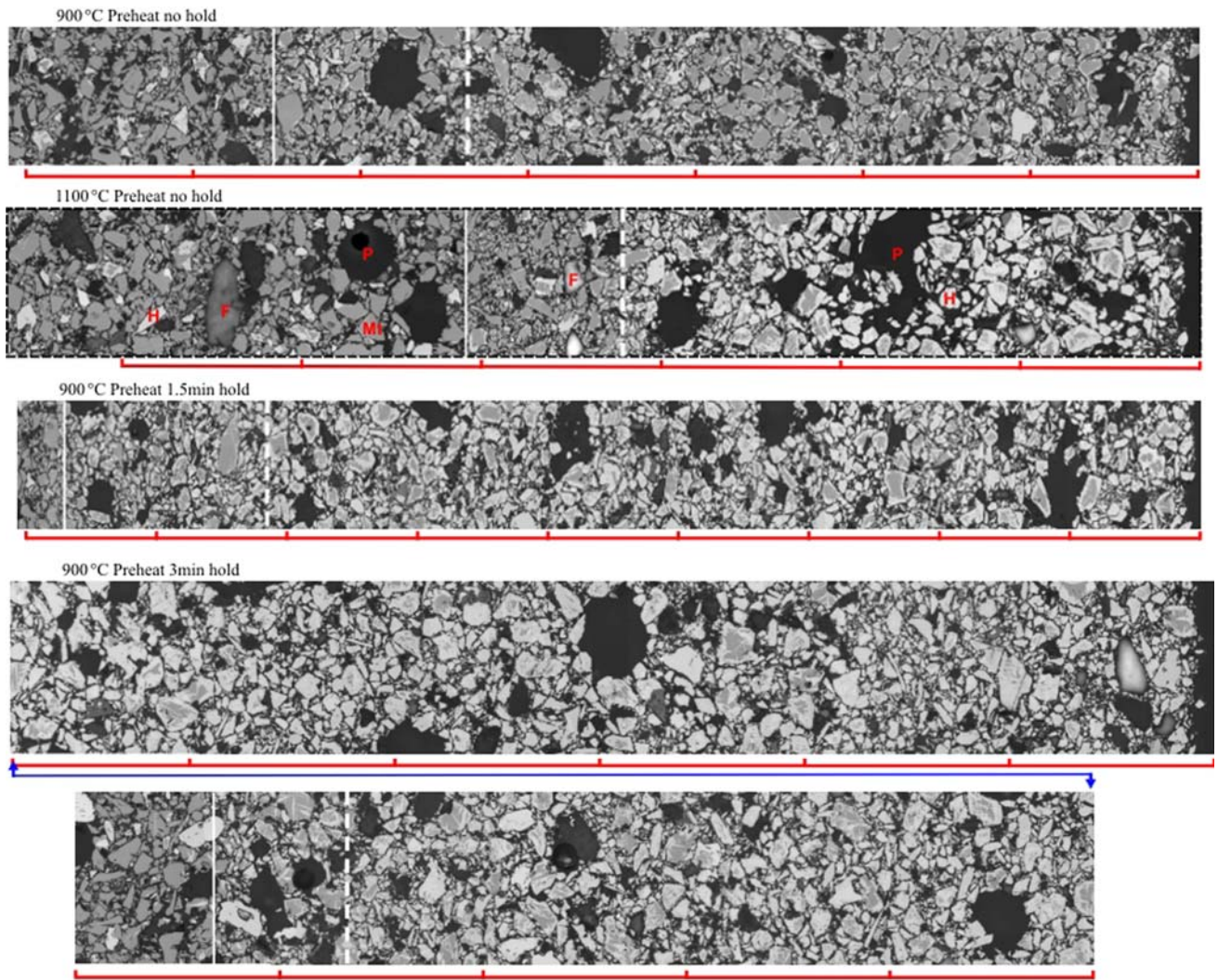


Fig. 5—Strip images taken in reflected light from the periphery (right side of image) toward the center of the pellet (left side of image) to just past the reacted zone (solid vertical line). Legend: *Mt* = magnetite, *H* = hematite, *F* = flux, *P* = pore space, dashed line = full oxidation of the mean 15- μm -sized particles. The ruler shown underneath each image is graduated in 250- μm steps. The two images for the sample preheated to 900 °C for 3 minutes are joined at the point indicated by the arrowed line.

of the particle.^[18] As iron ore pellets are similarly porous to limestone particles, a similar diffusion-controlled calcination reaction can occur when sufficient limestone is present to generate sufficient CO_2 in the pellet pore space to reach the equilibrium concentration.

In Figures 5 and 6, the extent of penetration of the oxidation front and calcination front, respectively, is shown for selected experiments as a line across the image. The penetration is then compared with the result generated by the mathematical model for the identical heating profile in Figure 7. In Figure 7, the solid black line represents the output of the mathematical model at a particular time in a temperature ramp for oxidation of magnetite particles across the radius of the pellet. These are compared with the experimentally determined oxidation of the magnetite particles. Because magnetite can become slightly oxidized before the crystal structure reverts to hematite,^[25] the maximum extent of this oxidation of magnetite, 6.6 pct, was shown as the

experimental extent of the oxidation front (or, more correctly, the hematite formation front) for comparison with the mathematical model. Because the mathematical model for magnetite oxidation assumed a uniform particle size of 15 μm , “full oxidation” was defined as the point where hematite penetrated 7.5 μm into the magnetite grains on average (*i.e.*, a particle of 15 μm would be just oxidized). The extent of full oxidation of idealized 15- μm magnetite grains is represented in Figure 5 by a broken white line across the image. The experimental extents of initial and full oxidation of magnetite are marked on Figure 7 with black diamonds. Figure 7 also shows the extent of calcination calculated by the model across the radius of the pellet as a dashed gray line. For pellets that were studied using the electron microprobe, an estimate of the penetration of the calcination front determined from the element maps and marked on Figure 7 as an open gray square.

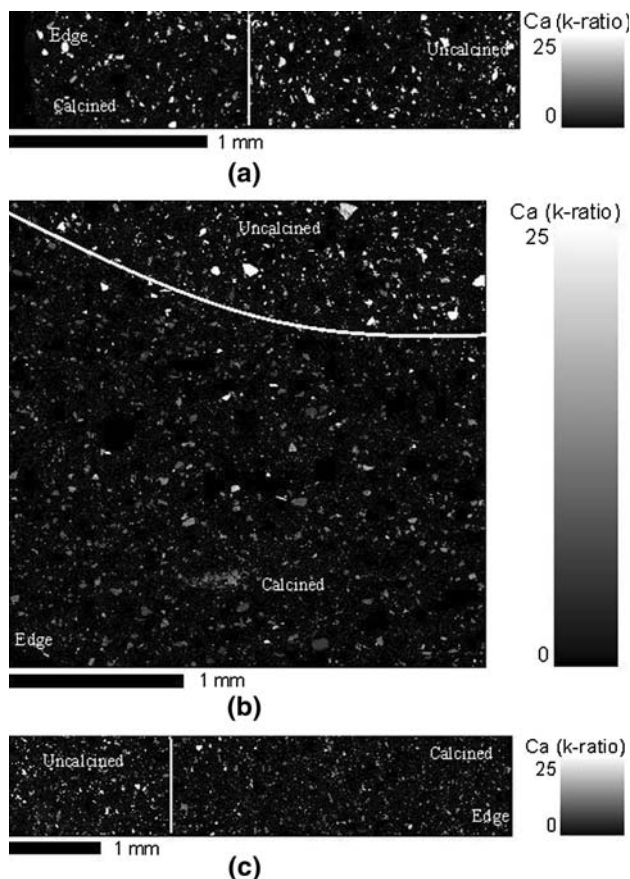


Fig. 6—EMPA map of calcium concentration for pellets heated to (a) 900 °C, (b) 1000 °C, and (c) 1100 °C and then quenched in liquid nitrogen.

Figure 7 shows that the results for magnetite oxidation from the mathematical model fit fairly well with experimental observations, particularly for the location of the initial oxidation front. Leaving out the effects on gas diffusion in the pellet from the carbon dioxide produced from flux calcination resulted in significant deviations from the experimental results for the penetration of the oxidation front (Figure 4). The mathematical model predicts a thicker reaction zone than was observed experimentally, however. In previous studies on magnetite oxidation,^[1–3,20] significant variation in oxidation kinetics have been found for different magnetite concentrates, most likely due to mineralogy differences between deposits. The slight difference between the intraparticle diffusion kinetics used in the model, determined by Mosen *et al.*^[20] for Sydvaranger concentrate, and the real kinetics for the concentrate used, could have led to this difference in reaction zone width. This small error in reaction zone width would have little impact on predictions for overall magnetite conversion within the pellet provided the estimate for volume mean magnetite particle size is accurate.

In Figure 7, the calcination front determined by the mathematical model did not penetrate as far as that determined experimentally for the samples studied with

EPMA. This was only experimentally significant for the pellet held at 1000 °C for 90 seconds. This error was probably due to the assumption of the MgCO_3 component of the dolomite decomposing with the same kinetics as the CaCO_3 . In reality, the MgCO_3 calcines at a slightly lower temperature, indicating slightly lower activation energy for that reaction. A more detailed model that deals with both steps in the decomposition of dolomite may provide a more accurate simulation of the movement of the calcination front within the pellet. The error in accurately locating the calcination front is not as important as locating the oxidation front, however, because the rate of oxidation of iron ore pellets has a greater impact on the final pellet properties.^[22,23,26]

D. Strategies for Accelerating Oxidation

On face value, additional grinding of the fluxes would appear to be a valid method of improving magnetite oxidation during preheating, because finer flux particles would react quicker. A simulation with the model was performed with the fluxes ground to a mean particle size of 6 μm instead of 15 μm . This resulted in no difference in the calcination or oxidation rates. This was because the diffusion rate of CO_2 out of the pellet is the limitation and the overall particle size and pellet porosity were largely unchanged. The individual carbonate particles did react quicker initially, but the volume of CO_2 generated was the same. This was validated by the experiments, which showed that calcite particles of different sizes appeared to react roughly simultaneously at the same level of penetration.

Higher porosity in the pellet (or, equivalently, less tortuosity) was shown to reduce the time necessary for oxidation (Figure 8). The difficulty with trying to improve average green ball porosity to improve magnetite oxidation on the grate is that the strength of the green balls would also be inferior. This could lead to green balls breaking up and clogging the pellet bed during preheating. If this occurred, the permeability of the pellet bed and hence heat transfer would be impaired, negating the benefits of reduced oxidation time with increased pellet porosity. A compromise between pellet oxidation and green ball strength would need to be determined by pot grate experiments for an individual pellet operation.

It is difficult to compare results generated by the mathematical model against experimental results due to the range of porosity exhibited between iron ore green balls and the tendency of green balls themselves to have lower porosity in the core compared to the outer shell.^[15] Figure 8 shows that variation in porosity by as little as 0.01 led to a 5 pct difference in the extent of magnetite oxidation at a particular time.

Modifying the grind size of the magnetite had mixed results in terms of improving the speed of oxidation in fluxed pellets, as can be seen in Figure 9. Initially, the larger grain size slows oxidation due to diffusion through the iron oxide grains being the controlling factor. Once the amount of carbon dioxide builds up in the system and the iron oxide grains have begun to oxidize, the larger grain size and the resultant larger

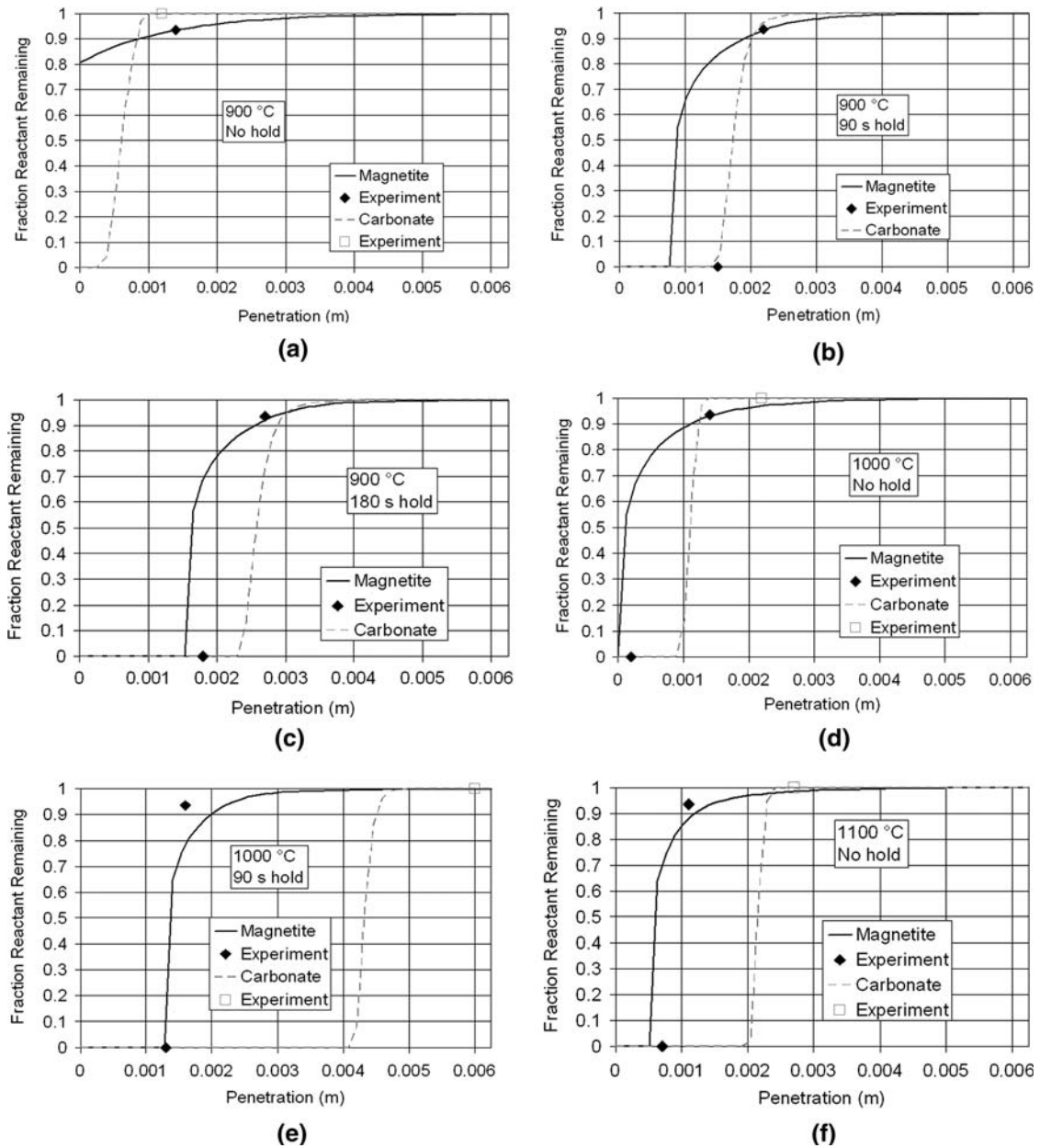


Fig. 7—Comparison of penetration of reaction fronts from the mathematical model and single pellet experiments for various times and temperatures.

pores allow both the CO_2 to escape the pellet quicker and oxygen to diffuse quicker to the oxidation front. This leads to the oxidation rate overtaking that of a pellet with a smaller grain size. Because producing magnetite concentrate at a coarser grind often leads to lower grades, sometimes unacceptably so, the improvement in magnetite oxidation during preheat may be accompanied by a loss of grade in the product pellet.

VI. CONCLUSIONS

This study has shown that models of fluxed magnetite pellet induration need to consider the diffusion of gas

species into and out of the pellet to achieve more accurate results. The currently used whole plant models^[6-8] have been shown to be inaccurate in the way they deal with magnetite oxidation and carbonate calcination in pellets. First, carbonate calcination has been shown, by both mathematical modeling and physical experiment, to undergo a shrinking core reaction and not simultaneous reaction across the pellet. This is due to the buildup in the pellet of CO_2 to its equilibrium concentration, limited by the rate of diffusion out of the pellets. More importantly, the carbon dioxide escaping the pellet after being generated by calcination interferes with oxygen migration to the shrinking core interface where magnetite oxidation is occurring. This leads to a

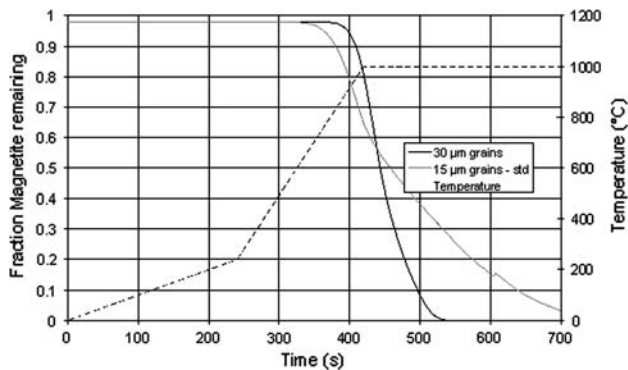


Fig. 8—Effect of increased mean magnetite particle size on magnetite oxidation for a heating profile typical of a preheated pellet. The sawtooth patterns on the oxidation curves are due to numerical instability in the simulation.

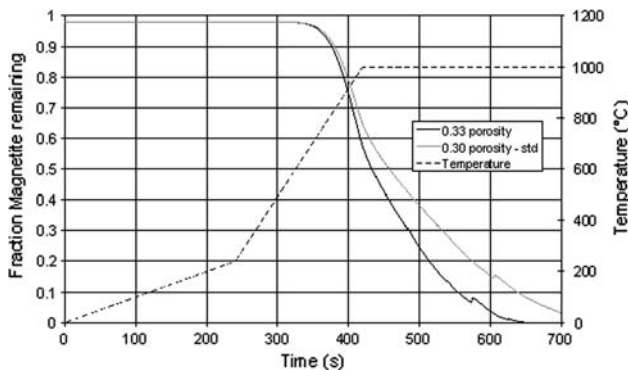


Fig. 9—Effect of increased porosity on magnetite oxidation for a heating profile typical of a preheated pellet. The sawtooth patterns on the oxidation curves are due to numerical instability in the simulation.

potential to further optimize the induration of fluxed magnetite pellets by selecting the best preheating conditions for the concentrate and flux combination. It is not just a case of determining “where to oxidize”^[26] but also “where to calcine” to minimize the impact of carbon dioxide generation on magnetite oxidation.

Unfortunately, the model developed here is not directly applicable to whole plant analysis models of pellet induration, because it would be too computationally intensive. This could perhaps be improved slightly by using a nonuniform adapting spatial grid that became smaller around the reaction interfaces (both oxidation and calcination). It was beyond the scope of this article, however, to determine the most computationally efficient solution method, and an approximation technique based on the current detailed model would probably be sufficient for inclusion in a whole plant induration model. This work will be followed up by further development and research using SIRO-Indur^[27] as a platform to investigate the effects on the whole plant of the updated pellet model presented here. Further fundamental work will also pursue a model for all reactions that occur during the induration of iron ore pellets using the current MATLAB model as a starting point.

ACKNOWLEDGMENTS

Jeff Douglas is acknowledged for his assistance with some of the experimental work using the infrared image furnace. Jean-Pierre Guerbois, University of Technology (Sydney), is thanked for performing the thermogravimetric analysis included in this work. Nick Wilson is thanked for performing the EPMA analysis of the pellets produced from the infrared image furnace. Liming Lu, Jonathan Campbell, and Warren Bruckard, CSIRO, are thanked for their assistance in reviewing drafts of this article.

NOMENCLATURE

C	concentration (mol/m ³)
D_{ss}	diffusion coefficient for oxygen ions through hematite (m ² /s)
k_{ox}	oxidation reaction constant (m/s)
r_g	instantaneous radius of magnetite within the iron oxide grain (m)
r_{go}	initial magnetite grain radius (m)
R_{ox}	rate of oxidation (mol/s)
S	local reactive surface area of limestone (m ² /kg)
S_o	initial reactive surface area of limestone (m ² /kg)
t	time (s)
X	conversion of carbonate (—)
$\Delta\rho_o$	stoichiometric density factor ^[1] (mol/m ³)

SUBSCRIPTS

eq	equilibrium
O_2	oxygen

REFERENCES

1. D. Papanastassiou and G. Bitsianes: *Metall. Trans.*, 1973, vol. 4, pp. 487–96.
2. P.O. Pape, R.D. Frans, and G.H. Geiger: *Ironmaking and Steelmaking*, 1976, vol. 3, pp. 138–45.
3. L. Bentell and G. Mathisson: *Scand J. Met.*, 1978, vol. 7, pp. 230–36.
4. S.E. Olsen and T. Malvik: *5th Int. Symp. Agglomeration*, IChemE, Rugby, United Kingdom, 1989, pp. 229–310.
5. L.A. Haas, J.C. Nigro, and R. Moe: *51st Ironmaking Conf. Proc.*, ISS, Warrendale, PA, 1992, pp. 533–49.
6. S. Caron, G. Ouellet, D. Roy, and G. Paquet: *59th Ironmaking Conf. Proc.*, ISS, Warrendale, PA, 2000, pp. 439–44.
7. M. Cross and P. Blot: *Metall. Mater. Trans. B*, 1999, vol. 30B, pp. 803–13.
8. J.A. Thurlby: *Metall. Trans. B*, 1988, vol. 19B, pp. 103–12.
9. A.R. Firth: *Trans. Inst. Min. Metall. C*, 2007, vol. 116, pp. 93–100.
10. H. Ohta, T. Akiyama, and I.-K. Suh: *Tetsu-to-Hagané*, 1989, vol. 75, pp. 1877–82.
11. J.C. Slattery and R.B. Bird: *AIChE J.*, 1958, vol. 4, pp. 137–42.
12. C.F. Curtis and J.O. Hirschfelder: *J. Chem. Phys.*, 1949, vol. 17, pp. 550–55.
13. J. Szekeley, J.W. Evans, and H.W. Sohn: *Gas Solid Reactions*, Academic Press, New York, NY, 1976, pp. 28–31.
14. G.M. Maizel', V.I. Klein, V.M. Abzalov, V.A. Tveritin, A.P. Butkarev, I.R. Vinokurova, Y.G. Yaroshenko, and V.P. Trofimov: *Steel USSR*, 1980, vol. 10, pp. 580–82.

15. M.-E. Boucher and J.-F. Wilhelmy: *Proc. Montreal Energy and Mines Conf.*, Canadian Institute of Mining and Metallurgy, Montreal, 2007, pp. 332–39.
16. J.R. Wynnnyckyj: *6th Int. Symp. on Agglomeration*, The Society of Powder Technology, Tokyo, Japan, 1993, pp. 143–59.
17. R.H. Borgwardt: *AIChE J.*, 1985, vol. 31, pp. 103–11.
18. A.B. Fuertes, G. Marban, and F. Rubiera: *Trans. IChemE*, 1993, vol. 71A, pp. 421–28.
19. D. Papanastassiou and G. Bitsianes: *Metall. Trans.*, 1973, vol. 4, pp. 477–86.
20. B.E. Monsen, S.E. Olsen, and L. Kolbeinsen: *Scand J. Met.*, 1994, vol. 23, pp. 74–80.
21. S.H. Kang, S.H. Chang, and H.I. Yoo: *J. Solid State Chem.*, 2000, vol. 149, pp. 33–40.
22. A.R. Firth, J.D. Douglas, and J.F. Garden: *4th Int. Congr. on the Science and Technology of Ironmaking*, Iron and Steel Institute of Japan, Tokyo, pp. 688–91.
23. A.R. Firth, J.F. Garden, and J.D. Douglas: *VIII Brazilian Symp. on Iron Ore*, Associação Brasileira de Metalurgia e Materiais, São Paulo, Brazil, 2007, pp. 689–99.
24. E.T. Turkdogan: *Physical Chemistry of High Temperature Technology*, Academic Press, New York, 1980, pp. 290–341.
25. E.J. Fasiska: *Corr. Sci.*, 1967, vol. 7, pp. 833–39.
26. V. Niiniskorpi: *61st Ironmaking Conf. Proc.*, ISS, Warrendale, PA, 2002, pp. 533–45.
27. A.R. Firth, D.B. Saunders, and S.C.T. Trang: *VI Brazilian Symp. on Iron Ore*, Associação Brasileira de Metalurgia e Materiais, São Paulo, Brazil, 2005, pp. 135–44.